Research Article | Vol. 26, No. 11 | 28 May 2018 | OPTICS EXPRESS 14201
Optics EXPRESS

Temporal characteristics of quantum cascade laser frequency modulated combs in long wave infrared and THz regions

NATHAN HENRY,[1,*] DAVID BURGHOFF,[2] QING HU,[2] AND JACOB B. KHURGIN[1]

[1]*Whiting School of Engineering, Johns Hopkins University, Baltimore, MD 21218, USA*
[2]*Department of Electrical Engineering and Computer Science, Research Laboratory of Electronics, Massachusetts Institute of Technology, Cambridge, Massachusetts 02139, USA*
[*]*nhenry7@jhu.edu*

Abstract: We consider here a time domain model representing the dynamics of quantum cascade lasers (QCLs) generating frequency combs (FCs) in both THz and long wave infrared (LWIR λ = 8-12μm) spectral ranges. Using common specifications for these QCLs we confirm that the free running laser enters a regime of operation yielding a pseudo-randomly frequency modulated (FM) radiation in the time domain corresponding to FCs with stable phase relations in the frequency domain. We provide an explanation for this unusual behavior as a consequence of competition for the most efficient regime of operation. Expanding the model previously developed in [Opt. Eng. 57(1), 011009 (2017)] we analyze the performance of realistic THz and LWIR QCLs and show, despite the vastly different scale of many parameters, that both types of lasers offer very similar characteristics, namely FM operation with an FM period commensurate with the gain recovery time and an FM amplitude comparable with the gain bandwidth. We also identify the true culprit behind pseudo-random dynamics of the FM comb to be spatial hole burning, rather than the more pervasive spectral hole burning.

OCIS codes: (140.5965) Semiconductor lasers, quantum cascade; (140.3518) Lasers, frequency modulated; (300.6340) Spectroscopy, infrared; (300.6495) Spectroscopy, terahertz.

References and links

1. T. Udem, R. Holzwarth, and T. W. Hänsch, "Optical frequency metrology," Nature **416**(6877), 233–237 (2002).
2. S. Diddams, "Optical frequency combs: Introduction, sources and applications," in Proceedings of IEEE International Frequency Control Symposium (IEEE, 2009)
3. A. Schliesser, N. Picqué, and T. W. Hänsch, "Mid-infrared frequency combs," Nat. Photonics **6**(7), 440–449 (2012).
4. M. Yu, Y. Okawachi, A. G. Griffith, M. Lipson, and A. L. Gaeta, "Mode-locked mid-infrared frequency combs in a silicon microresonator," Optica **3**(8), 854–860 (2016).
5. G. Ycas, F. R. Giorgetta, E. Baumann, I. Coddington, D. Herman, S. A. Diddams, and N. R. Newbury, "High-coherence mid-infrared dual-comb spectroscopy spanning 2.6 to 5.2 μm," Nat. Photonics **12**(4), 202–208 (2018).
6. J. Faist, F. Capasso, D. L. Sivco, C. Sirtori, A. L. Hutchinson, and A. Y. Cho, "Quantum cascade laser," Science **264**(5158), 553–556 (1994).
7. J. Faist, G. Villares, G. Scalari, M. Rösch, C. Bonzon, A. Hugi, and M. Beck, "Quantum cascade laser frequency combs," Nanophotonics **5**(2), 272–291 (2016).
8. D. E. Spence, P. N. Kean, and W. Sibbett, "60-fsec pulse generation from a self-mode-locked Ti:sapphire laser," Opt. Lett. **16**(1), 42–44 (1991).
9. S. Barbieri, M. Ravaro, P. Gellie, G. Santarelli, C. Manquest, C. Sirtori, S. P. Khanna, E. H. Linfield, and A. G. Davies, "Coherent sampling of active mode-locked terahertz quantum cascade lasers and frequency synthesis," Nat. Photonics **5**(5), 306–313 (2011).
10. C. Y. Wang, L. Kuznetsova, V. M. Gkortsas, L. Diehl, F. X. Kärtner, M. A. Belkin, A. Belyanin, X. Li, D. Ham, H. Schneider, P. Grant, C. Y. Song, S. Haffouz, Z. R. Wasilewski, H. C. Liu, and F. Capasso, "Mode-locked pulses from mid-infrared Quantum Cascade Lasers," Opt. Express **17**(15), 12929–12943 (2009).
11. D. Burghoff, T.-Y. Kao, N. Han, C. W. I. Chan, X. Cai, Y. Yang, D. J. Hayton, J.-R. Gao, J. L. Reno, and Q. Hu, "Terahertz laser frequency combs," Nat. Photonics **8**(6), 462–467 (2014).
12. A. Hugi, G. Villares, S. Blaser, H. C. Liu, and J. Faist, "Mid-infrared frequency comb based on a quantum cascade laser," Nature **492**(7428), 229–233 (2012).

#326697 https://doi.org/10.1364/OE.26.014307
Journal © 2018 Received 3 Apr 2018; revised 9 May 2018; accepted 9 May 2018; published 21 May 2018

Optics EXPRESS

13. G. Villares, A. Hugi, S. Blaser, and J. Faist, "Dual-comb spectroscopy based on quantum-cascade-laser frequency combs," Nat. Commun. **5**, 5192 (2014).
14. Y. Yang, D. Burghoff, D. J. Hayton, J.-R. Gao, J. L. Reno, and Q. Hu, "Terahertz multiheterodyne spectroscopy using laser frequency combs," Optica **3**(5), 499–502 (2016).
15. J. Khurgin, Y. Dikmelik, A. Hugi, and J. Faist, "Coherent frequency combs produced by self frequency modulation in quantum cascade lasers," Appl. Phys. Lett. **104**(8), 081118 (2014).
16. N. Henry, D. Burghoff, Y. Yang, Q. Hu, and J. B. Khurgin, "Pseudorandom dynamics of frequency combs in free-running quantum cascade lasers," Opt. Eng. **57**(1), 011009 (2017).
17. M. S. Vitiello, G. Scalari, B. Williams, and P. De Natale, "Quantum cascade lasers: 20 years of challenges," Opt. Express **23**(4), 5167–5182 (2015).
18. S. Kumar, Q. Hu, and J. L. Reno, "186 K operation of terahertz quantum-cascade lasers based on a diagonal design," Appl. Phys. Lett. **94**(13), 131105 (2009).
19. S. Kohen, B. S. Williams, and Q. Hu, "Electromagnetic modeling of terahertz quantum cascade laser waveguides and resonators," J. Appl. Phys. **97**(5), 053106 (2005).
20. D. Burghoff, T.-Y. Kao, D. Ban, A. W. M. Lee, Q. Hu, and J. Reno, "A terahertz pulse emitter monolithically integrated with a quantum cascade laser," Appl. Phys. Lett. **98**(6), 061112 (2011).
21. D. Burghoff, C. Wang Ivan Chan, Q. Hu, and J. L. Reno, "Gain measurements of scattering-assisted terahertz quantum cascade lasers," Appl. Phys. Lett. **100**(26), 261111 (2012).
22. H. Choi, L. Diehl, Z.-K. Wu, M. Giovannini, J. Faist, F. Capasso, and T. B. Norris, "Gain recovery dynamics and photon-driven transport in quantum cascade lasers," Phys. Rev. Lett. **100**(16), 167401 (2008).
23. B. Gelmont, V. Gorfinkel, and S. Luryi, "Theory of the spectral line shape and gain in quantum wells with intersubband transitions," Appl. Phys. Lett. **68**(16), 2171–2173 (1996).
24. N. Owschimikow, C. Gmachl, A. Belyanin, V. Kocharovsky, D. L. Sivco, R. Colombelli, F. Capasso, and A. Y. Cho, "Resonant second-order nonlinear optical processes in quantum cascade lasers," Phys. Rev. Lett. **90**(4), 043902 (2003).
25. T. Aellen, M. Beck, N. Hoyler, M. Giovannini, J. Faist, and E. Gini, "Doping in quantum cascade lasers. I. In Al As–In Ga As/ In P midinfrared devices," J. Appl. Phys. **100**(4), 043101 (2006).
26. K. Fujita, S. Furuta, A. Sugiyama, T. Ochiai, T. Edamura, N. Akikusa, M. Yamanishi, and H. Kan, "High-Performance Quantum Cascade Lasers With λ~8.6 μm Single Phonon-Continuum Depopulation Structures," IEEE J. Quantum Electron. **46**(5), 683–688 (2010).
27. S. Kočinac, S. Tomić, Z. Ikonić, and V. Milanović, "Gain optimization in electrically pumped AlGaAs quantum cascade lasers," J. Opt. Soc. Am. B **19**(10), 2357–2364 (2002).
28. C. Gmachl, F. Capasso, J. Faist, A. L. Hutchinson, A. Tredicucci, D. L. Sivco, J. N. Baillargeon, S. G. Chu, and A. Y. Cho, "Continuous-wave and high-power pulsed operation of index-coupled distributed feedback quantum cascade laser at λ≈ 8.5 μ m," Appl. Phys. Lett. **72**(12), 1430–1432 (1998).
29. J. B. Khurgin, Y. Dikmelik, P. Q. Liu, A. J. Hoffman, M. D. Escarra, K. J. Franz, and C. F. Gmachl, "Role of interface roughness in the transport and lasing characteristics of quantum-cascade lasers," Appl. Phys. Lett. **94**(9), 091101 (2009).
30. G. Villares and J. Faist, "Quantum cascade laser combs: effects of modulation and dispersion," Opt. Express **23**(2), 1651–1669 (2015).
31. D. Burghoff, Y. Yang, D. J. Hayton, J.-R. Gao, J. L. Reno, and Q. Hu, "Evaluating the coherence and time-domain profile of quantum cascade laser frequency combs," Opt. Express **23**(2), 1190–1202 (2015).

1. Introduction

Frequency combs [1, 2], initially developed in the near-infrared and visible domains, have changed the world of metrology and spectroscopy as we know it. They have been used to demonstrate extremely quick data acquisition, with favorable sensitivity and resolution. There has now been a strong push to extend the spectral range of FCs down to the UV, up to mid and far IR regime, and even out to THz. Infrared and THz regimes are of particular interest due to the fact that many molecules possess strong fundamental resonances in this domain, giving spectroscopic access to a wide variety of molecules. Additionally, atmospheric windows lie in the IR and THZ giving the potential to detect trace gasses of environmental or toxic vapors down to concentrations of parts-per-billion. Unfortunately, FC access to the long-wave and THz regimes have been hindered by lack of viable sources. Typically, generation of FCs in the mid-to-far IR are a result of frequency conversion which is inherently inefficient leading to small powers in the range of 1nW/mode [3]. Furthermore, frequency combs are typically generated using mode-locked lasers, micro-resonators and optical downconverters greatly adding to the complexity, power consumption, and size of the spectroscopic tool [4, 5]. To avoid this complexity a logical choice would be to turn to electrically pumped lasers, which for the LWIR and THz regions implies Quantum Cascade

Optics EXPRESS

lasers (QCLs) [6, 7], which, while barely 20 years old, have already become a ubiquitous source of coherent radiation in these ranges. By analogy with other lasers [8], one would expect to obtain FCs by mode locking the QCL and obtaining a train of short pulses whose spectrum is a FC, however this turns out to be far more difficult than it seems. Passive mode-locking is next to impossible to achieve in QCLs because of their inherently short gain recovery time, due to fast non-radiative times of intersubband transitions (ISTs), on the order of ~1ps when compared to the round trip time on the order of τ_{rt}~100ps. Active mode-locking has been achieved for QCL's [9, 10], however with pulse width well above theoretical predictions. Moreover, active mode-locking cannot reach the bandwidth that could be provided by a passive mode-locking regime of operation.

Despite all these pessimistic predictions, not only has consistent QCL FC operation from mid IR to THz been demonstrated [11, 12] but it has already been used in spectroscopy [13, 14]. Experiments have shown that, given proper dispersion compensation and a broadband gain medium, free running QCLs do operate in the FC regime and they do it without any additional intra-cavity nonlinear elements (such as saturable absorbers, Kerr lenses etc.). Furthermore, the observed QCL FC's were quite different from all other FC's in the sense that rather than producing trains of ultra-short pulses in time domain their output power was almost constant in time while the frequency of oscillation was modulated, hence a stable phase relation between the oscillating modes existed. This relation is maintained by four wave mixing (FWM) in the fast saturable, intersubband gain medium of QCL.

While the performance of today's QCL FCs is sufficient for many practical applications in spectroscopy, it still suffers from a number of issues. Comb lines and beat notes between them suffer from prominent hysteretic behavior and are hard to predict. The breadth of FC can be narrow, to the detriment of the dynamic range of the spectroscopic tool, and often times erratic jumps in the beat notes can be seen [7]. To better understand this behavior, it is necessary to develop a more complete description of the device's operating dynamics. Previously a theoretical model was developed in the frequency domain (FD) [15], illustrating that frequency modulation is indeed a natural consequence of spatial hole burning in broad gain medium, which causes the laser to favor multimode operation, combined with the short gain recovery time which favors constant intensity. Obviously, a comb-like spectrum combined with the nearly constant intensity is a signature of FM operation.

But the character of FM predicted by the aforementioned model was rather unexpected to the observer who may be used to smooth periodic FM signals used in communication or radars. While on the longer time scale (~100ps) the FM was obviously periodic with a period equal to τ_{rt}, within this period the FM was totally aperiodic with some average modulation period, T_{FM}, which is commensurate with the laser gain recovery time, τ_2. Within the period, the FM signal appeared entirely random and not repeatable each time the model was cold started and the lasing developed from noise. However, once the model settled into this "pseudo-random" (PR) regime the character of FM did not change. Experiments have also confirmed that while FC's do not correspond to smooth periodic signals, they are remarkably resilient [12].

It is this remarkable PR FM time domain (TD) characteristic of QCL FCs that we attempt to explain in this paper, while improving upon the FD model [15] by incorporating an inhomogeneous gain and, as a result, spectral hole burning. As a first step, the time domain model has been recently developed in [16] using Optical Bloch Equations and the derivation there have shown that as long as the period of FM is substantially longer than coherence time of the gain medium (0.2ps for LWIR and 0.7ps for THz) one can use a rate equation approximation and thus greatly reduce complexity of calculations. We now apply this model to realistic THz and LWIR lasers in order to conclusively explain why the FM does appear pseudo-random. We find that while FM by itself does a great job in filling in spectral holes,

Optics EXPRESS

the reason behind the PR nature is found in spatial hole burning. By mitigating hole burning the QCL is able to lower its threshold, thus this regime of operation prevails.

2. Pseudo-random FM in frequency domain

Presented in Fig. 1(a) is the simplified model for the QCL gain medium used in this paper, the gain occurs between upper (ULL) and lower (LLL) laser levels with non-radiative relaxation occurring at a rate of τ_2^{-1}. Electrons are injected into the ULL by tunneling through a barrier at rate of τ_t^{-1}, they then proceed to provide gain and are subsequently recycled into the next period by relaxing (usually via sequential phonon emission) from the LLL into the injector of the next period [17]. In Fig. 1(b) we illustrate how two counter-propagating waves inside the cavity will interfere to create an intensity pattern, to be discussed further later. Shown in Fig. 1(c) are three possible (out of an infinite number) steady state solutions for the instant frequency deviation as a function of time, normalized to τ_{rt}, and obtained using FD model developed in [15]. The signals share roughly the same FM amplitudes and mean periods however, they appear entirely uncorrelated otherwise, and thus pseudo random. It is readily apparent that both signals repeat after reaching the cavity round trip time, hence the instant FM signal is strongly aperiodic within τ_{rt}, yet repeats every τ_{rt}. The FM optical field is described as $E(t) = E_o \exp[i\int \omega(t)dt]$ where E_0 is a constant amplitude and $\omega(t)$ is the instant frequency oscillating around the central (carrier) frequency ω_0, with amplitude $2\pi A_{FM}$, i.e. $|\omega(t) - \omega_0| \le 2\pi A_{FM}$.

Prior to engaging in detailed TD analysis let us first consider a simple phenomenological picture that sheds light on how FM operation reduces threshold and increases power efficiency of THz and LWIR QCLs. In Fig. 1(d) we present a figure of the QCL material gain saturation (both THz and LWIR) with and without FM. In this figure, the FM signal used is not random but rather a simple sinusoid with period equal to the gain recovery time and an amplitude commensurate with the bandwidth of the gain. Note that the gain profile for a THz laser in Fig. 1(d) is much higher and narrower than for LWIR, see Fig. 1(d), this is namely due to a much larger dipole moment (gain scales to the square of the dipole moment) as well as longer ULL lifetimes in THz QCLs, due to the increased diagonality of the IST [18]. This higher gain is required for the THz laser as the waveguide free carrier absorption is much higher in this domain. Although it may not be perfectly discernible in the graph (as we show below the relative changes on gain dynamics imposed by the character of the FM are small but sufficient for one of the FM regimes to become the stable operational regime), the gain remaining after passing light through the gain medium is greater when no FM is present, amounting to an inefficient use of the spectral gain. Without the frequency modulation a deep spectral hole is burned in the center of the gain, to the detriment of the laser operation. Additionally, all the gain on the sides of the hole is lost to nonradiative relaxation at a rate equal to the reciprocal inverse of the gain recovery time. Now, if the frequency is modulated multiple modes are introduced into the cavity and one can predict a more uniform use of the gain. Frequency modulation accomplishes two goals: firstly, it allows for the spectrally inhomogenous gain to recover as the FM signal detunes from its resonance, filling spectral holes; secondly, it reduces the occurrence of two counter-propagating waves meeting with similar frequencies, thus smoothing spatial holes and peaks in the gain profile. This means that, with frequency modulation, more energy is directed to stimulated emission and hence the threshold is lower, and the amount of energy "wasted" to non-radiative relaxation decreases. Thus, this regime of operation is bound to emerge as a result of competition.

Optics EXPRESS

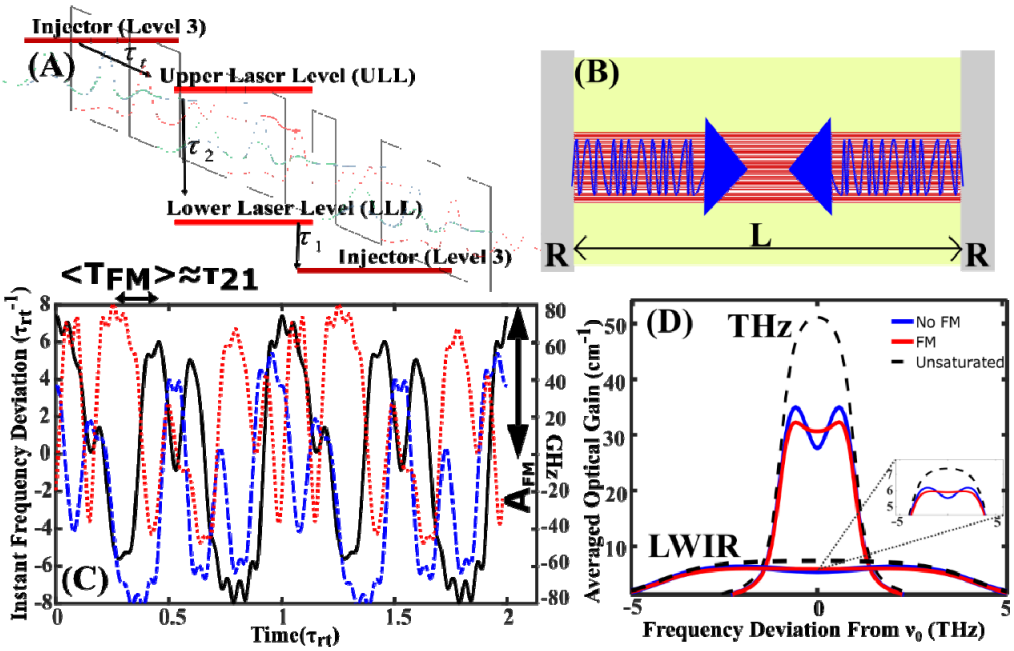

Fig. 1. (a) Simplified level definitions of our 3-level QCL model. (b) Cavity diagram of two counter-propagating, frequency modulated waves, the background of which illustrates the cladding and active layers. (c) Pseudo random frequency modulation obtained from the model developed in [15], each signal is generated from a separate run. (d) Spectral gain profile of THz and LWIR QCLs with and without FM.

3. FM and Interplay of spatial and spectral hole burning

While the simple FD model explains why FM modulation is desirable and even why it should occur with a period commensurate with τ_2, what it does not explain is why the signal is always aperiodic on a small scale within one round trip time, τ_{rt}. Let us consider an intuitive picture of why randomness is so important. In Fig. 2 we show the instant frequency for five different FM signals (column 1), their spectra (column 2) and the power density distribution inside the laser cavity (column 3) of length $L = v_g \tau_{rt} / 2$, where v_g is the group velocity. The power density profiles are the result of the addition of two counter-propagating waves, in other words the light interfering with a delayed (by $\Delta t = 2z / v_g$, $0 < \Delta t < T_c$) version of itself,

$$I(z,t) = \left| A_1(z)E(t + \Delta t/2)e^{j(kz-\omega_0 t)} + A_2(z)E(t - \Delta t/2)e^{-j(kz+\omega_0 t)} \right|^2, \quad (1)$$

where

$$E(t) = E_0 \exp\left(-i\int \omega_{FM}(t)dt\right), \quad (2)$$

and the normalized amplitudes $A_1^2(z) = [2R + (2-2R)z/L]/(1+R)$ and $A_2^2(z) = [2-(2-2R)z/L]/(1+R)$ account for the boundary conditions at the edges with reflectivity R. For LWIR, R~30% was calculated for an uncoated facet using Fresnel formula. However, for THz QCL's R is typically much higher, 70-80%, this is due to the metal-metal waveguide structure and impedance mismatch at the cavity facet [19]. Importantly, because the gain medium does not saturate instantly we use the power density averaged over the gain

Optics EXPRESS

recovery time, or $\langle I(z,t)\rangle_{\tau_2} = \tau_2^{-1}\int_0^{\infty} I(z,t-\tau)\exp(-\tau/\tau_2)d\tau$. Let us now see how the character of FM affects the gain saturation.

For the non-FM signal, $\omega_{FM}(t) \equiv \omega_0$ shown in upper row (Fig. 2(a)), one can see that in addition to the previously mentioned spectral hole, the spatial hole is also expected to be burned as the intensity represents a standing wave pattern of peaks and troughs as shown in the last column. In the next row (Fig. 2(b)), the frequency is modulated with a period equal to the round trip time, $\omega_{FM}(t) = \omega_0 + 2\pi A_{FM}\sin(2\pi t/\tau_{rt})$, hence all the modes are present in the spectrum as shown in the second column. The spatial intensity pattern $\langle I(z,t)\rangle_{\tau_2}$ in Fig. 2(b) column 3 shows greatly reduced swing of the oscillation since the instant frequencies of two counter-propagating waves are always different except at the mirrors, thus no spatial hole burning is expected. While prospects look bright in the spatial domain, the performance is not that great in the FD. As stated before, FM allows for the gain at some frequency to recover as the radiation detunes from its resonance. However, after the gain recovers at the rate τ_2^{-1}, further pumping is converted into non-radiative decay. Thus, for efficient operation, the radiation must return to its original frequency within the gain recovery time (τ_2). In other words the period of FM modulation, T_{FM}, must be on the order of the gain recovery time, indicating that the FM signal shown in Fig. 2(b) is far from optimum.

On the other end of the scale one can consider the FM signal whose modulation period T_{FM} is commensurate with τ_2, $\omega_{FM}(t) = \omega_0 + 2\pi A_{FM}\sin(2\pi tm/\tau_{rt})$, where $m \sim \tau_{rt}/\tau_2$ (Fig. 2(c)). This signal produces lines separated by a much larger spacing than τ_{rt}^{-1}, contrary to FCs seen in experiment. For THz lasers, $m \sim 25-50$ meaning that every 25 to 50 modes are skipped, this situation is even worse for LWIR QCLs where τ_{rt}/τ_2 is larger by one order of magnitude. It is intuitively clear that the larger the number of oscillating modes, the more efficiently can the spatial hole be filled. It can be understood even better by realizing that when two counter-propagating waves, delayed by time Δt, interfere inside the cavity they have instant frequencies that differ by some fixed amount, $\Delta\omega(z)$, hence the standing wave pattern moves with the velocity $v_{pat}(z) \sim \lambda\Delta\omega(z)/4\pi n_{eff}$. As long as $v_{pat}(z)\tau_2 > \lambda/2n_{eff}$, i.e. $\Delta\omega(z) > 2\pi\tau_2^{-1}$, the spatial troughs and peaks will be smoothed out and averaged giving an intensity $\langle I(z,t)\rangle_{\tau}$ with a fairly flat profile. However, when $z \sim KL/m$, where K is an integer less than m, the two interfering waves are delayed by exactly $\Delta t \sim KT_{FM}$ and thus have nearly identical instant frequencies, causing a non-moving standing wave pattern peak in the intensity profile. Given a deterministic, sinusoidal FM signal, one can derive the z-dependent averaged intensity as

$$\langle I(z,t)\rangle_{\tau} = E_0^2\left[1 + J_0\left(\frac{A_{FM}\tau_{rt}}{m}\sin m\pi z/L\right)\cos(4\pi z/\lambda)\right] \qquad (3)$$

where $J_0(x)$ is a Bessel function of the first kind giving $m = \tau_{rt}/T_{FM}$ peaks of intensity variations along the cavity length. From (3) it is obvious that whenever the argument of the Bessel function is zero, the swings of the intensity reach a maximum creating an undesirable standing wave pattern.

In the presence of pseudo random FM, the counter-propagating waves rarely have matched frequencies for the time period comparable to τ_2 hence the interference pattern does not stay in place but essentially oscillates back and forth, getting smoothed out. To quantify these observations we introduce a "degree of randomness", $0 < \delta < 1$, into the expression for

Optics EXPRESS

instant frequency $\omega_{FM} = 2\pi A_{FM} \sin\left[\bar{\omega}_m (1+\delta R_t)t\right]$, where $\bar{\omega}_m = 2\pi / \bar{T}_{FM}$ is the mean angular frequency of the modulation, and $-1 \le R_t \le 1$ is a time dependent random number. To assure continuity of instant frequency the model generates a new number every $2[1+\delta R_t]^{-1}$, or after a half period of time has passed leading to the instant frequency changing. This is shown in the right hand columns of Figs. 2(d) and 2(e) with $\delta = 0.5$ and 0.9 respectively. As shown in the second columns of these figures, increasing the PR nature of the FM effectively spreads the spectrum, while keeping the separation of τ_{rt}^{-1}, due to its periodic nature. Importantly, the averaged intra-cavity intensity pattern shown in the last column is smooth and thus unlikely to cause significant spatial hole burning.

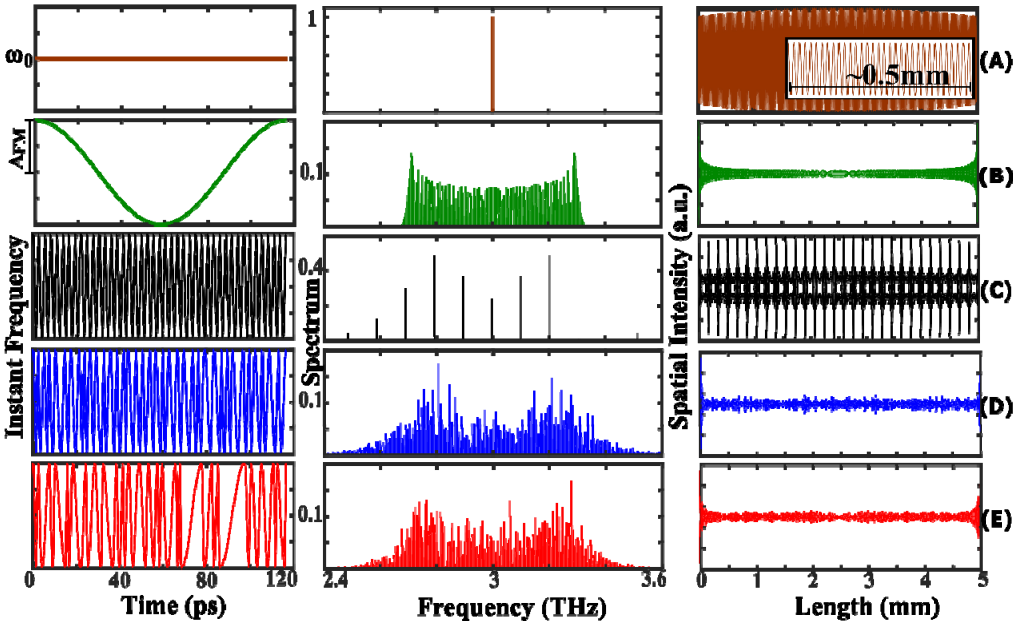

Fig. 2. Instant frequency deviation, power spectrum, and spatial distribution for an intracavity field with (a) no frequency modulation (b) non-random frequency modulation with a modulation period equal to the cavity round-trip time, (c)non-random frequency modulation with a period equal to the gain recovery time, (d) random frequency modulation, ($\delta = 0.5$) with mean period equal to the gain recovery time, (e) very random frequency ($\delta = 0.9$) modulation. Data presented here are for a QCL at 3 THz with a frequency modulation spanning 2 THz (A_{FM} = 1THz), further specifications follow that in Table 1 for a THz QCL.

4. Time domain study of FM FC operation

Now that we have developed an intuitive rational for the pseudo-random character of FM modulation we need to further quantify the effect and see if the FC characteristics are different for THz and LWIR QCLs. As shown in Fig. 1(a), the QCL active region can be represented as three levels described as: the injection level (level 3), upper laser level 2 (ULL), the lower laser level 1 (LLL), and followed by the injection level again in the next period. The lifetime of the ULL is τ_2^{-1}, depopulation of the LLL is achieved at a rate τ_1^{-1} and injection into the ULL from level 3 is at a tunneling rate τ_t^{-1}. While there are typically more than 3 levels in a QCL, such as stacked injector levels as well as levels that act as a buffer between depopulation and injection, we account for this by defining the depopulation time τ_1 in this model as the effective time it takes for an electron to transport from one period to the

Optics EXPRESS

next, without counting τ_t and τ_2. The TD model outlined here tracks the population dynamics of the laser using a set of simple rate equations that take into effect detuning of the radiation from resonance as a function of time, due to FM. As explained in [16] as long as the FM period is substantially larger than coherence time τ_{coh}, the gain dynamics can be approximated by the set of balance equations for the relative (as a fraction of total sheet doping density per period N_D) population inversion $N_{21}^{(n)}$ of the n-th group of the ISTs that are centered on some resonant frequency $\omega^{(n)}$ and the following equation can be derived:

$$\frac{d}{dt}N_{21}^{(n)}(z,t)=\frac{2N_o}{\tau_2}-\frac{2N_{21}^{(n)}(z,t)}{\tau_2}\left[1+I(z,t)/I_{sat}^{(n)}(t)\right], \tag{4}$$

where $I(z,t)$ is the intensity, $I_{sat}^{(n)}(t)=\dfrac{\bar{n}\hbar(1+\tau_{coh}^2\Delta\omega^{(n)}(t)^2)}{\tau_2 z_{21}{}^2 4\pi\alpha_o}$ is the saturation intensity which is time dependent following the time-dependent detuning $\Delta\omega^{(n)}(t)=\omega^{(n)}(t)-\omega_0$, τ_{coh} is the coherence time, z_{21} is the dipole moment between ULL and LLL, and α_0 is the fine structure constant. The gain spectrum is then calculated by weighing the population inversion spectrum with a normalized, super-Gaussian distribution function $f^{(n)}=f(\Delta\omega^{(n)})$ shown in Fig. 1b. This way the inhomogeneous component of spectral broadening is caused not only by the unintentional growth variation between periods and in plane, but also by a deliberate introduction of inhomogeneity in the periods.

Now, as the QCL is typically ran by a DC source, the current density J is constant through each broadened transition. Before lasing, each spectral bin is pumped to the population inversion equal to $N_0=J(\tau_2-\tau_1)/qN_D$. Once the lasing commences both the tunneling time, τ_t, and the depopulation time, τ_1, change as voltage increases assuring that the current remains continuous. For THz QCLs, with typical doping densities on the order of $3x10^{10}\,cm^{-2}$ and depopulation times on the order of a few picoseconds, we see that indeed expected current densities are within the range of 500-800 A/cm^2. In LWIR QCLs doping densities are higher $\sim 1x10^{11}\,cm^{-2}$, and the ISTs in them are more direct resulting in a much shorter depopulation times, in the sub-picosecond range. This yields typical current density values around an order of magnitude higher for LWIR than THz QCLs.

5. Numerical results and discussion

Now that we have developed the means to characterize various FM shapes and the set of equations to describe the laser dynamics, we can introduce the FM signals into the cavity and run equations to obtain the values of the "mean single pass gain" experienced by the signal $\bar{\gamma}=\langle\gamma(z,t)\rangle$ where under the rate equation approximation mentioned earlier,

$$\gamma(z,t)=\Gamma\sum_n f^{(n)}\frac{4\pi\alpha_0}{n_{eff}}\frac{N_D}{W}\frac{z_{21}{}^2\omega_o\tau_{coh}N_{21}^{(n)}(z,t)}{1+\tau_{coh}^2\Delta\omega^{(n)}(t)^2}, \tag{5}$$

W being the effective thickness of one active period, and n_{eff} the effective index is approximately equal to the material index. We additionally obtain the "nonradiative relaxation current density",

$$\bar{J}_{rel}=\left\langle qN_D\tau_2^{-1}\sum_n f_n N_2^{(n)}(z,t)\right\rangle_{z,t}, \tag{6}$$

essentially the fraction of total current density that relies on phonon rather than photon emission. Please refer to [1] for a derivation of Eqs. (4)-(6). In this case N_2 represents the

Optics EXPRESS

population on the ULL rather than population inversion. Obviously, a large average gain and complimentarily small J_{rel} would indicate that this particular regime has lower threshold, higher efficiency, and should be the preferred mode of laser oscillation.

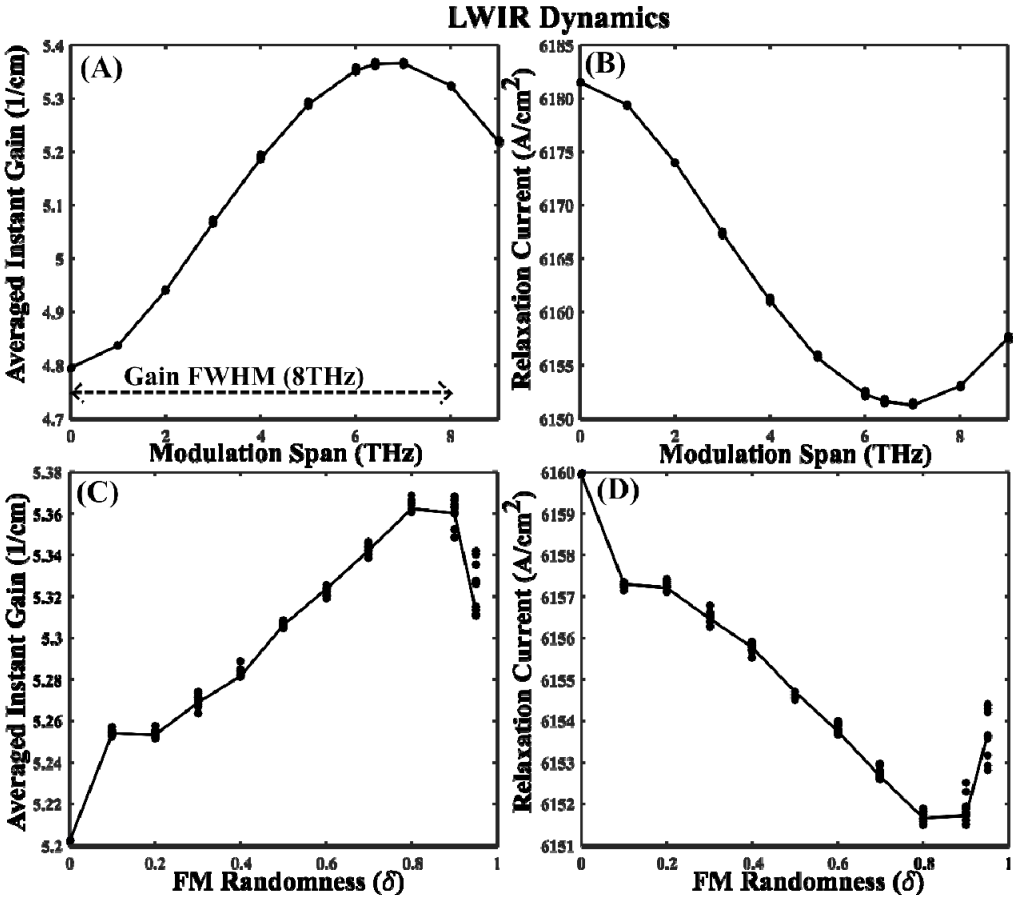

Fig. 3. Averaged instant gain (a and c) and relaxation current (b and d) versus frequency modulation span and randomness (δ) for an LWIR QCL.

Optics EXPRESS

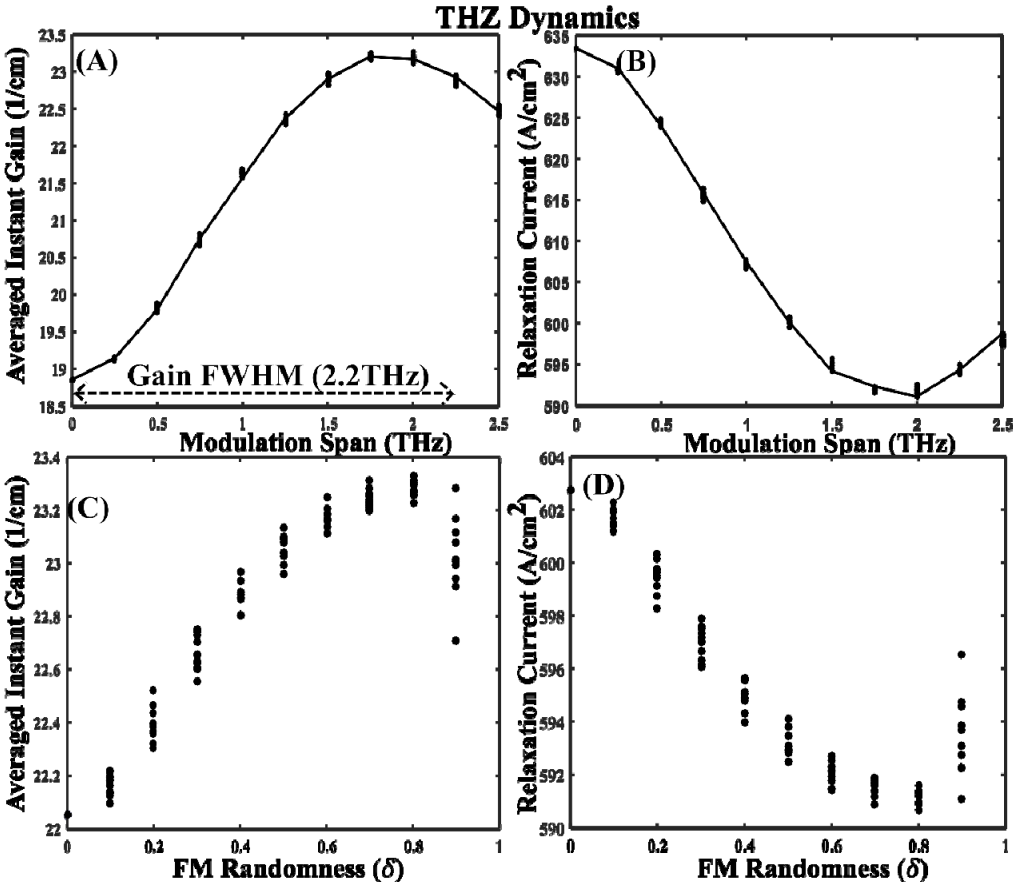

Fig. 4. Averaged instant gain (a,c) and relaxation current (b,d) versus frequency modulation span and randomness (δ) for a THz QCL.

Table 1. Laser specifications

f_0 (THz)	Current Density (A/cm^2)	$N_{2D}(cm^2)$/ W(nm)	τ_{coh} (ps)	τ_2	τ_1	z_{21} (nm)	P (mW)	P_{sat}	Cross section (μm^2)	Gain FWHM (THz)
3	800	$3.5x10^{10}$ /57	0.7	4	1.5	4.7	50	94.5	250	2.2
30	$6.4x10^3$	$4x5x10^{10}$ /68*	0.2	0.4	0.3	2.2	250	$3.4x10^3$	90	8

*The QCL laser simulated contains four $5x10^{10}$ cm^{-2}, delta doped layers per period.

We can now see how these calculations can become time consuming, especially for LWIR devices due to a much shorter wavelength than THz. For the LWIR model the number of spatial intervals $\Delta z \sim \lambda/10$ at which the spatial shape of the intensity must be calculated exceeds 7000. Additionally, the number of temporary intervals $\Delta t \sim \tau_2/10$ required to adequately describe the FM shape is 2000 and the number of spectral bins needed to faithfully reproduce the gain shape is 80. Thus, each 7000 x 2000 x 80 array corresponds to just one data point in Fig. 3. Furthermore, due to the random nature of the FM signal at least ten data points are required for each combination of δ and A_{FM}. Fortunately, our previous work [16] allows us to use rate equation approximation in place of full OBE solution which might have rendered the modeling unsurmountable with our modest computational power.

Optics EXPRESS

For the data presented in Figs. 3 and 4 a pseudo random instant frequency dependence $\omega(t)$ has been generated as described by (2) for each combination of δ and A_{FM}, with a mean period $\overline{T}_{FM}$ equal to τ_2. The electric field has been numerically delayed and summed with itself to create the interference pattern according to (1). This information is plugged into Eq. (4), and the final results evaluated using (5) and (6) are presented in Figs. 3 and 4 below. The graphs in Figs. 3 and 4 are generated using common specifications for QCLs in the LWIR and THz regimes respectively. Specifications, given in Table 1, were obtained from the references [11, 18, 20–29]. Both devices are modeled to be 2mm long, shorter than typical devices, however proven to be long enough to illustrate properly all the trends described below.

The graphs showing effective gain $\overline{\gamma}$ and nonradiative current density $\overline{J}_{rel}$ vs modulation span $(2A_{FM})$ have been produced using the optimum value of $\delta = 0.8$. QCL graphs with randomness for the x-axis are produced using the optimum modulation span, 6.2THz for LWIR and 1.8 THz for THz QCLs. As expected, both δ and A_{FM} reach their optimum values and the average gain experienced by photons increases and stimulated emission leaves fewer carriers to experience non-radiative relaxation to the LLL, confirming that the laser has reached optimum efficiency.

The key result that can be inferred from Figs. 3 and 4 is the importance of randomness. As we mentioned above, non-random FM ($\delta = 0$) goes a long way to decrease spatial hole burning when compared to a single frequency scenario, however, there still exist $m = \tau_{rt} / T_{FM}$ locations in the cavity where the modal frequencies between the two counter-propagating waves match creating peaks and troughs in the gain. By introducing randomness into the FM signal, the stationary standing wave pattern is suppressed as the two waves no longer meet with similar frequencies, or at the least it does not last very long and the gain does not see the instant intensity but rather the average over the upper state lifetime, this scenario does not cause spatial holes. Of course, when δ approaches unity the change of instant frequency can become too slow (in comparison to τ_2) causing the appearance of spectral holes, hence the optimum value of δ is always less than unity. The shape of the spatial hole burning depends heavily on the modulation index, in our case A_{FM} / ω_{FM}. Thus, while an optimum FM signal must span close to the entire spectral gain at a rate of $1/\tau_2$, the fact that the spatial distribution depends heavily on the ratio between the two will broaden the set of possible FM signal solutions. This further confirms our inference that there exists an infinite number of solutions for the laser's FM signal.

Other than the large difference in gain, as explained earlier, both THz and LWIR show very similar trends. Comparing averaged instant gain values between no frequency modulation and an optimum, pseudo-random FM regime, the LWIR experienced an increase of 0.6 cm^{-1} while the THz laser improved by 4 cm^{-1}. This disparity in improvement is easily reconciled by finding the percentage of improvement relative to the unsaturated gain, in this case both lasers have improved by 8%, a small percentage yet enough to influence the laser's operation. It is of note that a larger improvement is in fact seen under full OBE modeling [16] suggesting that we could be slightly underestimating the gain increase. Regarding the drop in relaxation current for both lasers, and using Eq. (6), we can calculate the decrease in wasted carriers and thus the direct increase in photons. Namely, the QCL experiences an increase in photons of $7\text{x}10^7$ cm^{-2} for LWIR and $1.1\text{x}10^9$ cm^{-2} for the THz laser, note we do not include loss other than through the mirrors. It should also be noted that the data point taken to be the most inefficient, and thus the data used as the base for comparison, might not be completely physical in the sense that this regime of operation, namely multi-mode with no FM or AM, would not occur. In fact, without FM the multi-mode laser would certainly exhibit amplitude modulation, which we have shown to decrease laser efficiency [16].

Optics EXPRESS

Prior to making the conclusions, we shall ascertain the practical applications of this work. While it is of vital importance to recognize the fundamental physics guiding the behavior of QCLs generating FCs, and it is our hope that furthering the understanding of the QCL FC community will help to incubate new methods for FC stability, we recognize that applying the results presented in this paper to actually design a QCL comb with improved performance is difficult. As has been shown via a frequency domain model [30], and numerous experimental papers, group velocity dispersion (GVD) is the main factor preventing formation of a wide and stable FC. Therefore, compensating the GVD remains the best route to broadband QCL combs. At this point we can also speculate that increasing mirror reflectivity makes spatial hole mitigation more important and thus in lasers with both mirrors having higher reflectivity the FC may be broader and more stable (at the expense of output coupling efficiency), however this hypothesis needs further testing. Additionally, the analysis presented here has illustrated that spatial hole burning is better mitigated by a large modulation index (A_{FM} / ω_{FM}). As the amplitude of modulation is commensurate with the gain spectral bandwidth, this implies that a broader gain spectrum may further improve stability of the laser.

6. Conclusion

We have thus presented a plausible explication of the physical processes behind the natural self-frequency modulating behavior displayed by the free running QCL in both THz and LWIR frequency ranges. The explanation presented centers around the ansatz that the most efficient form of operation will have the lowest lasing threshold, and thus will be the one in which a free running laser will settle; rather than any other operating regime. As the laser begins to oscillate, the inhomogeneously broadened gain of the QCL naturally tends toward multimode operation, subsequently four wave mixing (FWM) creates and locks these modes. To prevent spectral hole burning, an inevitable consequence of an inhomogeneously broadened gain, the QCL self-frequency modulates its radiation keeping intensity nearly constant to avoid fast saturation of the gain in time domain. Yet another deleterious mechanism of spatial hole burning still exists in the FM laser and in this work we had shown conclusively that when FM is pseudo-random within one round trip time the standing wave pattern causing spatial holes gets washed away, making this FM regime the most efficient one. Our model has yielded the optimum values of mean FM period commensurate with gain recovery time, the FM span commensurate with gain bandwidth and very strong randomness of modulation which agrees with the experimental data [31] as well as with FD model [15]. It is interesting to note that despite very diverse parameters for LWIR and THz QCLs, both devices show a marked improvement in operation when introduced to a pseudo random frequency modulation spanning roughly the gain spectral bandwidth at a rate equal to the upper state lifetime. We have therefore shown that given a partially inhomogeneously broadened, fast saturable gain of QCLs, and a tendency to suppress spatial hole burning, this pseudo-random FM regime is a completely natural operating mode for the QCL no matter what its lasing wavelength.

Funding

DARPA SCOUT program.

Acknowledgement

The authors acknowledge generous support provided by DARPA SCOUT program. Additionally, JK would like to thank Prof. Jérôme Faist's group at ETH for hosting him on sabbatical leave and for many stimulating discussions.